Switching of Magnons by Electric and Magnetic Fields in Multiferroic Borates

A. M. Kuzmenko,[1] D. Szaller,[2] Th. Kain,[2] V. Dziom,[2] L. Weymann,[2] A. Shuvaev,[2] Anna Pimenov,[2] A. A. Mukhin,[1] V. Yu. Ivanov,[1] I. A. Gudim,[3] L. N. Bezmaternykh,[3,*] and A. Pimenov[2]

[1]*Prokhorov General Physics Institute, Russian Academy of Sciences, 119991 Moscow, Russia*
[2]*Institute of Solid State Physics, Vienna University of Technology, 1040 Vienna, Austria*
[3]*L. V. Kirensky Institute of Physics Siberian Branch of RAS, 660036 Krasnoyarsk, Russia*

(Received 18 August 2017; published 12 January 2018)

Electric manipulation of magnetic properties is a key problem of materials research. To fulfill the requirements of modern electronics, these processes must be shifted to high frequencies. In multiferroic materials, this may be achieved by electric and magnetic control of their fundamental excitations. Here we identify magnetic vibrations in multiferroic iron borates that are simultaneously sensitive to external electric and magnetic fields. Nearly 100% modulation of the terahertz radiation in an external field is demonstrated for $SmFe_3(BO_3)_4$. High sensitivity can be explained by a modification of the spin orientation that controls the excitation conditions in multiferroic borates. These experiments demonstrate the possibility to alter terahertz magnetic properties of materials independently by external electric and magnetic fields.

DOI: 10.1103/PhysRevLett.120.027203

The continuous development of electronic devices drives the necessity to obtain an electric control of magnetic effects [1,2]. Compared to external magnetic field, electric voltage may be applied to a smaller spatial area and with much less switching power, thereby improving the performance and increasing the density of integrated components. In recent years, a substantial contribution to achieving electric manipulation of magnetic properties [2] has been realized through the application of multiferroics (i.e., materials with simultaneous electric and magnetic ordering) [3–7]. In several multiferroics, the coupling between electricity and magnetism is strong enough to allow a mutual influence of both properties. This magnetoelectric coupling has been demonstrated to lead to manipulation of magnetic moments [8–14] and magnetic structures [15–18] by an external electric field. These effects have been shown to survive up to room temperature [19,20]. Recent reviews of the topic can be found in Refs. [1,2,21].

Having in mind possible applications, the time scale of switching is an important issue. For example, in typical ferroelectric devices, this time is limited by the speed of domain wall propagation, which sensitively depends upon the amplitude of the electric field [22] and may be as short as a few tenths of nanoseconds [23–26]. In multiferroics, the problem of fast switching is not fully settled. Because of low static electric polarization in spin-driven multiferroics [6,27], substantial degradation of the switching time has been reported [28]. Extremely short switching times of electric polarization and magnetization can be reached using pulsed laser light. Depending on the specific mechanism of the interaction of the light pulse and the spins, the switching time may be within 40 fs [29]. Several interesting recent developments in the field of light-matter interaction include spin modulation via thermalization processes [30], pumping the energy into the electronic transitions [31], using the magnetic component of a terahertz pulse [32], or directly exciting the magnetoelectric excitation in a multiferroic material [33]. Detailed discussion of the experiment and theory of the short-time optical manipulation of magnetism is given in Refs. [29,34,35].

Besides the electric modification of static magnetic structures, a control of the high-frequency properties is of substantial interest [36]. To accomplish this control in practice, the dynamic processes, which are sensitive to the influence of the static electric field, have to be identified. Especially for terahertz light, the multiferroics are promising, as they possess magnetoelectric excitations allowing the combination of electric and magnetic fields. These excitations are called electromagnons [37–39] and an external magnetic field may easily change them. However, until now, only a few experiments could demonstrate the electric control of excitations in multiferroics [40,41]. Similar to static experiments, the control here is achieved by modifying the electric domain structure with the gate voltage. In addition, ferromagnetic resonance in ferromagnetic thin films has been demonstrated to be sensitive to static voltage [42–45]. The mechanism of the last effect is generally attributed to the voltage dependence of the magnetic anisotropy. In this work, we utilize another route to electric control of dynamic magnetic properties based on an influence of electric and magnetic fields on the spin orientation that determines the excitation conditions of fundamental magnetic modes.

Rare-earth iron borates represent one exotic class of multiferroics [46–48]. At high temperatures, all rare-earth borates reveal a noncentrosymmetric trigonal structure

belonging to the space group $R32$ [49–52], which persist down to lowest temperatures for Sm- and Nd-iron borates [53]. The connection between magnetic and electric ordering in iron borates is realized via the coupling of electric polarization to the antiferromagnetically ordered spin lattice [54–58].

Without losing any generality, we consider $SmFe_3(BO_3)_4$ below. As an approximation, the magnetoelectric coupling in iron borates with easy-plane antiferromagnetic order may be written in the symmetry-dictated form [54–56]

$$P_x \sim L_x^2 - L_y^2. \quad (1)$$

Here, P_x is the electric polarization along the crystallographic a axis and $L_x = M_{1x} - M_{2x}$ and $L_y = M_{1y} - M_{2y}$ are the x, y components of the antiferromagnetic vector of the ordered iron moments. Here, the magnetic structure is modeled by two antiferromagnetically coupled sublattices $\mathbf{M}_1$ and $\mathbf{M}_2$, respectively. A peculiarity of Eq. (1) is because $SmFe_3(BO_3)_4$ is an easy-plane antiferromagnet. We note that, in high enough magnetic fields, the antiferromagnetic vector realigns perpendicular to the field (i.e., $\mathbf{L} \perp \mathbf{H}$). In agreement with Eq. (1), for the $\mathbf{H} \| b$ axis, one obtains [55] $L_x \neq 0$, $L_y = 0$, $P_x > 0$, and for the $\mathbf{H} \| a$ axis, $L_x = 0$, $L_y \neq 0$, $P_x < 0$. That is, the electric polarization rotates by 180° after a 90° rotation of the external magnetic field.

In zero field, the magnetic moments of different domains or regions are distributed approximately homogeneously, as illustrated schematically in Fig. 1(a), thus averaging the electric polarization to zero. The magnetic fields as weak as 0.5 T are enough to break the homogeneous distribution, which leads to a nonzero electric polarization [47,54–56] according to Eq. (1) and Figs. 1(c) and 1(e). This effect is quadratic in small magnetic fields and may be described as a first order magnetoelectric effect. Because of the symmetry of the magnetoelectric coupling [59], the opposite effect must be possible as well: the magnetization must be sensitive to an external electric field. Indeed, such sensitivity has been recently demonstrated [60,61] in static experiments for $SmFe_3(BO_3)_4$ and $NdFe_3(BO_3)_4$.

Multiferroic iron borates present a rich collection of excitations in the terahertz range [62–65]. According to the optical experiments [66,67], in the iron borates the splitting of the ground rare-earth doublets are close to the magnon frequencies of the magnetic Fe subsystem. Therefore, not only the static properties of the iron borates are strongly influenced by the rare earth [54–56,58], but also the magnetic modes in these systems are strongly coupled. The last effect is seen experimentally as, e.g., a redistribution of the mode intensities and shifts of the resonance frequencies [62,63].

Our experiments revealed that only coupled Fe–rare-earth modes show measurable sensitivity to static electric fields. The strongest effect has been detected for the Sm-Fe mode around 10 cm^{-1}. In case of $SmFe_3(BO_3)_4$, other modes [62] may be also expected to reveal voltage

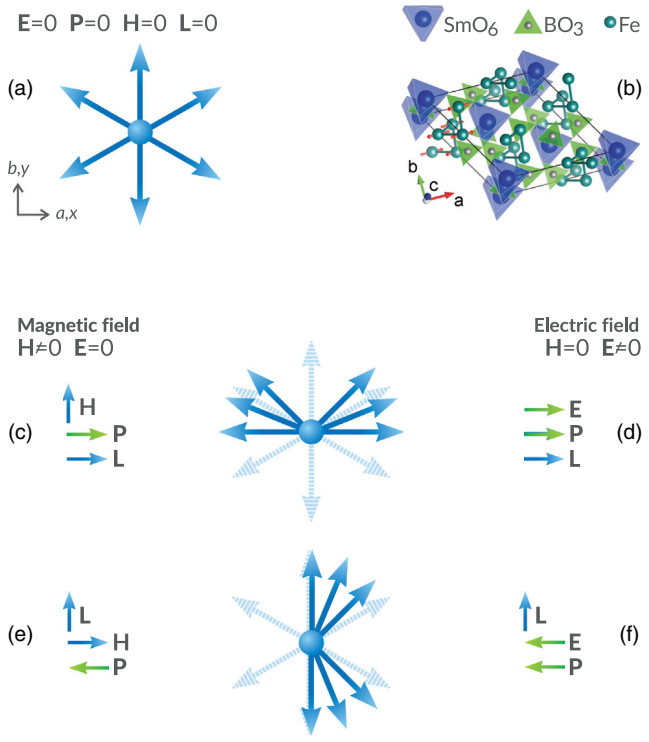

FIG. 1. Electric and magnetic ordering in rare-earth iron borates. (a) Homogeneous distribution of Fe spins (blue arrows) in the ab plane and in the absence of static magnetic ($\mathbf{H}$) and electric ($\mathbf{E}$) fields. Different arrows refer to different domains in the sample. Both antiferromagnetic vector $\mathbf{L}$ and static polarization $\mathbf{P}$ equal zero in this case. (c),(d) Either magnetic field $\mathbf{H} \| b$ (c) or electric field $\mathbf{E} \uparrow\uparrow a$ (d) induce $\mathbf{P} \uparrow\uparrow a$ and $\mathbf{L} \| a$. (e),(f) Rotation of the magnetic field to $\mathbf{H} \| a$ (e) or inversion of the electric field to $\mathbf{E} \uparrow\downarrow a$ (f) leads to the inversion of the static polarization and the rotation of the antiferromagnetic vector. Figure 1(b) shows the crystal structure of $SmFe_3(BO_3)_4$.

sensitivity. For the low-frequency electromagnon [64,65], a strong static magnetic field must be applied to raise the resonance frequency up to the millimeter frequency range. The magnetic field thus would align the Fe moments (see Fig. 1), suppressing the voltage effect. The mode around 14 cm^{-1} is too weak to reveal observable modulation. The high-frequency mode of Sm around 16 cm^{-1} has the wrong excitation conditions ($h \| c$ axis) for which it is not sensitive to a rotation of spins in the ab plane. In the case of $NdFe_3(BO_3)_4$, for the Fe mode around 4 cm^{-1}, no effect could be observed due to the weakness of this excitation.

Terahertz transmission experiments were carried out using quasioptical terahertz spectroscopy [53,68,69]. Single crystals of $SmFe_3(BO_3)_4$ and $NdFe_3(BO_3)_4$ with typical dimensions of ~1 cm were grown by crystallization from the melt on seed crystals as described in Ref. [70].

In $SmFe_3(BO_3)_4$, the coupled Fe-Sm antiferromagnetic mode around 10 cm^{-1} is of purely magnetic character and it may be excited by an ac magnetic field perpendicular to the antiferromagnetic $\mathbf{L}$ vector [62,63]. In the notations of Fig. 1(a) and without external fields, the local magnetic

moments are homogeneously distributed in the ab plane. This means that an average of 50% of magnetic moments is excited for any orientation of the ac magnetic field in the ab plane. The situation changes drastically if external magnetic or electric fields within the ab plane are present. As demonstrated in Figs. 1(c)–1(f), external fields destroy the homogeneous distribution of the magnetic moments in the ab plane. In the experiment, this breaks the balance between the excitation conditions with $\mathbf{h}\|a$ and $\mathbf{h}\|b$, respectively, thus shifting the mode intensity to one or the other direction ($\mathbf{h}$ and $\mathbf{e}$ refer to the oscillating magnetic and electric field of light, respectively).

The control of the observed mode intensity by an external magnetic field is shown in Fig. 2, where Figs. 2(a) and 2(b) demonstrate that the mode strength may be either suppressed or increased depending on the direction of the external magnetic field. As the fields above 0.5 T are sufficient to orient the magnetic moments fully, the intensity of the mode is either saturated at the doubled value compared to the $\mathbf{H} = 0$ case [Fig. 2(b)] or it is suppressed to zero [Fig. 2(a)]. As follows from the scheme of Fig. 1 and as demonstrated experimentally [47,55], in both cases, either positive or negative static electric polarization is observed along the crystallographic a axis.

The coupling of electric polarization with an external magnetic field in multiferroic iron borates provides the main idea how to control the magnetic excitations by an electric voltage. By different configurations shown in Fig. 1, the application of a static voltage along the a axis would favor one of the two possible orientations of the electric polarization. Simultaneously with the static magnetic configurations, the excitation conditions for the selected coupled Sm-Fe mode are changed, which may be employed for electric field control of the dynamic magnetic properties.

The basic results on electric field control of the magnetic excitation in $SmFe_3(BO_3)_4$ are shown in Fig. 3. In addition to the magnetic field dependence presented in Fig. 2, close to the resonance position of about 9.5 cm^{-1} we observe strong dependence both of the transmittance amplitude and of the phase shift in the electric fields of ~2.5 kV/cm. Particularly in the case of transmittance amplitude, we observe more than one order of magnitude changes in the terahertz signal as influenced by the electric field.

In spite of the large spectral changes close to the resonance frequency, far from the resonance we observe no measurable changes in the signal. This is because the contribution of the present magnetic mode, shown in Fig. 3(d), is small as compared to unity, the relative magnetic permeability of vacuum. In the scale of Fig. 3(b), the changes of the optical length of the sample far below the resonance can be estimated as $\Delta l \sim 1 \times 10^{-2}$ mm, which is below the sensitivity of the setup. On the other hand, the $\Delta\mu = 3.4 \times 10^{-3}$ contribution of the resonance under study and the increase of $\Delta\mu$ in higher fields agrees with the behavior of the static susceptibility [71]. The electric field modulation of magnetic susceptibility in the dynamic regime $d(\Delta\mu)/dE \approx 4 \times 10^{-7}$ cm/V is directly connected to the static magnetic susceptibility via $d(\Delta\mu)/dE = d\chi_y/dE_x$. The static values in $SmFe_3(BO_3)_4$ were recently measured [60] giving $d\chi_y/dE_x = 2.5 \times 10^{-8}$ cm/V, which is about an order of magnitude lower. The simplest explanation of this deviation

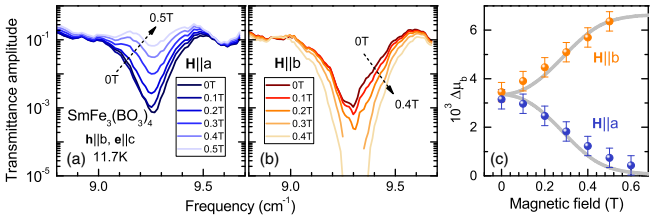

FIG. 2. Manipulation of magnon excitation by magnetic field. (a) Suppression of the magnon at 9 cm^{-1} in $SmFe_3(BO_3)_4$ by external magnetic fields along the a axis. (b) Increasing of the mode intensity in magnetic fields $\mathbf{H}\|b$ axis. (c) Magnetic field dependence of the mode intensity from fitting the spectra in Figs. 2(a) and 2(b) by a Lorentzian function (blue and orange spheres, respectively) and from model calculation based on Eq. (2) (solid gray lines).

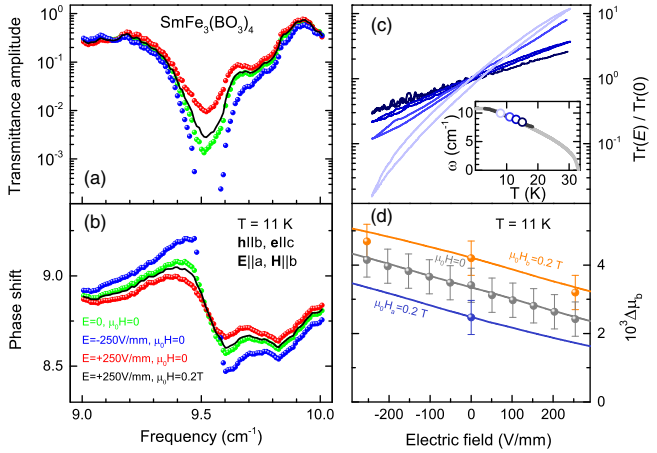

FIG. 3. Manipulation of the magnon in $SmFe_3(BO_3)_4$ by static electric field. (a) Transmittance amplitude and (b) phase shift spectra in the electric field. Symbols: green, initial state; blue, negative electric field; and red, positive electric field. The black line demonstrates that an external magnetic field can approximately compensate the effect of the electric field. (c) Direct modulation of the transmittance amplitude signal by a static electric field at different frequencies. The inset shows the temperature dependence of the resonance frequency as observed (dark gray line) and calculated (light gray line) in Ref. [62]. The temperatures and frequencies of the transmittance amplitude measurements are marked in the inset by circles. (d) Changes in magnon contribution in the electric field. Symbols are experimental results, while the solid lines come from model calculation based on Eq. (2). The orange and blue symbols correspond to a simultaneous application of electric and magnetic fields.

would be to attribute the static result to the sample twinning, which leads to the suppression of the magnetoelectric signal. However, other mechanisms, such as domain wall motion, cannot be excluded.

The influence of electric and magnetic fields on the magnetic mode contribution $\Delta\mu_y \sim \Delta\mu_0\langle L_x\rangle^2$ is determined by the square of the x component of the antiferromagnetic moment $\langle L_x\rangle^2$, averaged over the sample. To clarify this effect in more detail, we analyzed the actual part of the Landau free energy corresponding to the vector $\mathbf{L} = (\cos\varphi, \sin\varphi, 0)$ in the xy plane [56] (vector components are considered in the x, y, z Cartesian basis)

$$\Phi(\varphi, E, H) = \frac{1}{6}K_6\cos 6\varphi - \frac{1}{2}K_{1u}\cos 2\varphi - \frac{1}{2}K_{2u}\sin 2\varphi - \frac{1}{2}\chi_\perp H^2\sin^2(\varphi - \varphi_H) - P_\perp(E_x\cos 2\varphi - E_y\sin 2\varphi). \quad (2)$$

Here the first term represents the crystallographic hexagonal anisotropy energy, while the second and third terms stand for the magnetoelastic anisotropy $K_{1u} \sim \sigma_{xx} - \sigma_{yy}$, $K_{2u} \sim \sigma_{xy}$, which are induced by the internal elastic stress of compression-elongation $(\sigma_{xx} - \sigma_{yy})$ and σ_{xy} in the ab plane of a real crystal. The fourth term determines the Zeeman energy due to the canting of the antiferromagnetic structure in the magnetic field $\mathbf{H} = H(\cos\varphi_H, \sin\varphi_H, 0)$ and results in $\varphi = \varphi_H \pm \pi/2$ when the magnitude of the magnetic field dominates the ab plane anisotropy and the effect of the electric field. The last term of Eq. (2) accounts for the magnetoelectric coupling, i.e., the interaction of the spontaneous polarization $\mathbf{P} = (P_\perp\cos 2\varphi, -P_\perp\sin 2\varphi, 0)$ with external electric fields. The amplitude of the spontaneous polarization is determined by the magnetoelectric coupling constant and the electric susceptibility as described in Refs. [53,56]. By minimizing the free energy and taking into account that the crystallographic hexagonal anisotropy is small [56] compared to other contributions in Eq. (2), one can find the local orientation of the vector $\mathbf{L}$ in the ab plane as a function of electric and magnetic fields

$$\tan 2\varphi = \frac{2K_{2u} - \chi_\perp H^2\sin(2\varphi_H) - 4P_\perp E_y}{2K_{1u} - \chi_\perp H^2\cos(2\varphi_H) + 4P_\perp E_x}. \quad (3)$$

Assuming random distribution of the magnetoelastic anisotropies K_{1u} and K_{2u} obeying a two-dimensional Gaussian curve, we have simulated the behavior of $\Delta\mu_y$ in magnetic and electric fields. These results are shown in Figs. 2(c) and 3(d), which demonstrate a good description of the experiment. The main parameters of the model were taken from Ref. [56] (mean square deviation of the anisotropy $\Delta K_{1u} = \Delta K_{2u} \approx 5.5\times 10^3$ erg/cm^3 and the transverse magnetic susceptibility $\chi_\perp = 1.2\times 10^{-4}$ cm^3/g), while the maximal value of the spontaneous electric polarization was taken as $P_\perp \approx -240\ \mu$C/m^2. This value is slightly lower than that observed in Refs. [55,56], likely due to a larger amount of crystallographic inversion twins in the enantiomorph crystal. Remarkably, according to Eq. (3), the simultaneous application of both $\mathbf{E}$ and $\mathbf{H}$ could lead to a compensation of their action as a result of an interrelation between them. For example, for $\mathbf{E}\|a$ and $\mathbf{H}\|b$, the compensation effect occurs according to $\chi_\perp H_y^2 + 4P_\perp E_x = 0$, which is in good agreement with our measurements for $E = +250$ V/mm and $\mu_0 H_b = 0.2$ T [Figs. 3(a), 3(b), and 3(d)].

Figure 4 shows typical results of electric field experiments in $NdFe_3(BO_3)_4$. Figure 4(a) demonstrates the temperature dependence of the transmittance amplitude at selected frequencies. Characteristic minima in these data correspond to a crossing of the temperature-dependent resonance frequency of the mode and the frequency of the experiment, as shown in the inset. These measurements were obtained with cooling at 1 K/min and the simultaneous sweeping of the gate voltage between -500 and $+500$ V at a rate of $\sim$0.1 Hz. The characteristic sawtooth profile of these curves demonstrates the nonzero effect of the electric field on this magnetic mode in $NdFe_3(BO_3)_4$. From the slopes shown in Fig. 4(c), the field-dependent susceptibility may be estimated as $d\chi_y/dE_x = 2.4\times 10^{-8}$ cm/V, which is an order of magnitude smaller than the same values from $SmFe_3(BO_3)_4$. This difference is due to a small value of the spontaneous electric polarization and to a larger threshold magnetic field to suppress the spiral

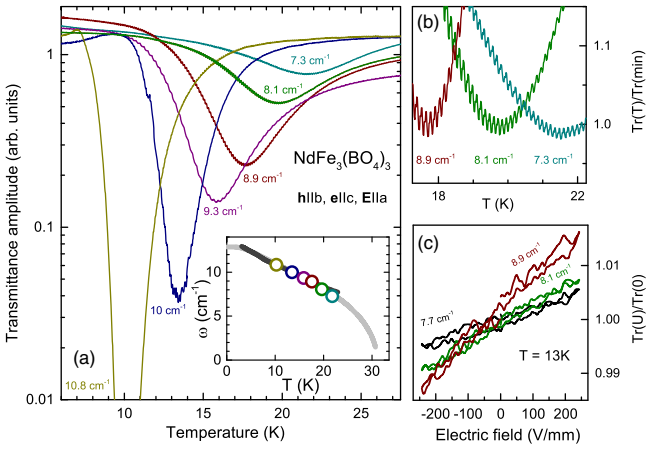

FIG. 4. Electric field effect in $NdFe_3(BO_3)_4$. (a) Temperature dependence of the relative transmittance amplitude signal for different frequencies. Weak sawtooth modulation of the curves is due to $\pm$500 V sweeping of electric voltage during the cooling process. The inset shows the temperature dependence of the resonance frequency as observed (dark gray line) and calculated (light gray line) in Ref. [62]. The temperatures and frequencies of the resonances seen in (a) are marked in the inset by circles. (b) An example of a detailed view of the data in (a). Here the spectra are normalized by the minimal transmitted intensity. (c) Direct modulation of the terahertz transmittance amplitude at selected frequencies in $NdFe_3(BO_3)_4$.

magnetic structure in $NdFe_3(BO_3)_4$ [~1 T compared to ~0.3 T for $SmFe_3(BO_3)_4$] [55,72].

The reaction time of the present experimental setup can be estimated as ~45 ms. Within this time scale, an instantaneous response of the magnetic system to the changes of the electric field have been observed. Based on the ac results given in Ref. [60], the switching times of at most 1 ms may be expected. As mentioned in the Introduction, in case of domain wall motion, the switching time of the devices are limited by tenths of nanoseconds. In magnetoelectric ferroborates, the process includes both rotation of the magnetic moments and switching of the electric polarization. The characteristic time scale for the magnetic part is determined by the in-plane antiferromagnetic resonance frequency (~5 GHz at $H = 0$) [64], which will probably determine the switching rate. Finally, for short pulses, electric and magnetic fields are present simultaneously. This mixing may influence the switching on the short time scales.

In conclusion, magnetic modes in multiferroic ferroborates are shown to be sensitive to both, external magnetic field and static voltage. Nearly 100% modulation of the terahertz radiation in an external electric field is demonstrated for $SmFe_3(BO_3)_4$. The experimental results can be well explained using a theoretical model that includes the magnetoelectric coupling in multiferroic borates. High sensitivity to electric voltage is due to a strong effect of both magnetic and electric fields on the spin orientation in an easy-plane antiferromagnetic structure and significant coupling of the rare-earth and the iron magnetic subsystems.

This work was supported by the Russian Science Foundation (16-12-10531: A. M. K., V. Yu. I., and A. A. M.), by the Russian Foundation for Basic Research (17-52-45091 IND-a: I. A. G. and L. N. B.), and by the Austrian Science Funds (W1243, I 2816-N27, I 1648-N27).

*Deceased.

[1] C. A. F. Vaz, J. Phys. Condens. Matter **24**, 333201 (2012).
[2] F. Matsukura, Y. Tokura, and H. Ohno, Nat. Nanotechol. **10**, 209 (2015).
[3] G. A. Smolenskii and I. E. Chupis, Sov. Phys. Usp. **25**, 475 (1982).
[4] M. Fiebig, J. Phys. D **38**, R123 (2005).
[5] S. Dong, J.-M. Liu, S.-W. Cheong, and Z. Ren, Adv. Phys. **64**, 519 (2015).
[6] Y. Tokura, S. Seki, and N. Nagaosa, Rep. Prog. Phys. **77**, 076501 (2014).
[7] M. Fiebig, T. Lottermoser, D. Meier, and M. Trassin, Nat. Rev. Mater. **1**, 16046 (2016).
[8] T. Lottermoser, T. Lonkai, U. Amann, D. Hohlwein, J. Ihringer, and M. Fiebig, Nature (London) **430**, 541 (2004).
[9] Y.-H. Chu, L. W. Martin, M. B. Holcomb, M. Gajek, S.-J. Han, Q. He, N. Balke, C.-H. Yang, D. Lee, W. Hu *et al.*, Nat. Mater. **7**, 478 (2008).
[10] M. Saito, K. Ishikawa, S. Konno, K. Taniguchi, and T. Arima, Nat. Mater. **8**, 634 (2009).
[11] Y. Tokunaga, N. Furukawa, H. Sakai, Y. Taguchi, T.-h. Arima, and Y. Tokura, Nat. Mater. **8**, 558 (2009).
[12] Y. J. Choi, C. L. Zhang, N. Lee, and S.-W. Cheong, Phys. Rev. Lett. **105**, 097201 (2010).
[13] Y. S. Oh, S. Artyukhin, J. J. Yang, V. Zapf, J. W. Kim, D. Vanderbilt, and S.-W. Cheong, Nat. Commun. **5**, 4201 (2014).
[14] M. Soda, S. Hayashida, B. Roessli, M. Månsson, J. S. White, M. Matsumoto, R. Shiina, and T. Masuda, Phys. Rev. B **94**, 094418 (2016).
[15] Y. Yamasaki, H. Sagayama, T. Goto, M. Matsuura, K. Hirota, T. Arima, and Y. Tokura, Phys. Rev. Lett. **98**, 147204 (2007).
[16] H. Murakawa, Y. Onose, and Y. Tokura, Phys. Rev. Lett. **103**, 147201 (2009).
[17] T. Finger, D. Senff, K. Schmalzl, W. Schmidt, L. P. Regnault, P. Becker, L. Bohaty, and M. Braden, Phys. Rev. B **81**, 054430 (2010).
[18] P. Babkevich, A. Poole, R. D. Johnson, B. Roessli, D. Prabhakaran, and A. T. Boothroyd, Phys. Rev. B **85**, 134428 (2012).
[19] T. Zhao, A. Scholl, F. Zavaliche, K. Lee, M. Barry, A. Doran, M. P. Cruz, Y. H. Chu, C. Ederer, N. A. Spaldin *et al.*, Nat. Mater. **5**, 823 (2006).
[20] D. M. Evans, A. Schilling, A. Kumar, D. Sanchez, N. Ortega, M. Arredondo, R. S. Katiyar, J. M. Gregg, and J. F. Scott, Nat. Commun. **4**, 1534 (2013).
[21] K. F. Wang, J.-M. Liu, and Z. F. Ren, Adv. Phys. **58**, 321 (2009).
[22] E. Fatuzzo, Phys. Rev. **127**, 1999 (1962).
[23] T. Tybell, P. Paruch, T. Giamarchi, and J.-M. Triscone, Phys. Rev. Lett. **89**, 097601 (2002).
[24] M. Dawber, K. M. Rabe, and J. F. Scott, Rev. Mod. Phys. **77**, 1083 (2005).
[25] A. Grigoriev, D.-H. Do, D. M. Kim, C.-B. Eom, B. Adams, E. M. Dufresne, and P. G. Evans, Phys. Rev. Lett. **96**, 187601 (2006).
[26] Y. Ehara, S. Yasui, T. Oikawa, T. Shiraishi, T. Shimizu, H. Tanaka, N. Kanenko, R. Maran, T. Yamada, Y. Imai *et al.*, Sci. Rep. **7**, 9641 (2017).
[27] S.-W. Cheong and M. Mostovoy, Nat. Mater. **6**, 13 (2007).
[28] T. Hoffmann, P. Thielen, P. Becker, L. Bohatý, and M. Fiebig, Phys. Rev. B **84**, 184404 (2011).
[29] A. Kirilyuk, A. V. Kimel, and T. Rasing, Rev. Mod. Phys. **82**, 2731 (2010).
[30] M. Matsubara, A. Schroer, A. Schmehl, A. Melville, C. Becher, M. Trujillo-Martinez, D. G. Schlom, J. Mannhart, J. Kroha, and M. Fiebig, Nat. Commun. **6**, 6724 (2015).
[31] S. L. Johnson, R. A. de Souza, U. Staub, P. Beaud, E. Möhr-Vorobeva, G. Ingold, A. Caviezel, V. Scagnoli, W. F. Schlotter, J. J. Turner *et al.*, Phys. Rev. Lett. **108**, 037203 (2012).
[32] T. Kampfrath, A. Sell, G. Klatt, A. Pashkin, S. Maehrlein, T. Dekorsy, M. Wolf, M. Fiebig, A. Leitenstorfer, and R. Huber, Nat. Photonics **5**, 31 (2011).
[33] T. Kubacka, J. A. Johnson, M. C. Hoffmann, C. Vicario, S. de Jong, P. Beaud, S. Grübel, S.-W. Huang, L. Huber, L. Patthey *et al.*, Science **343**, 1333 (2014).

[34] A. V. Kimel, A. Kirilyuk, F. Hansteen, R. V. Pisarev, and T. Rasing, J. Phys. Condens. Matter **19**, 043201 (2007).

[35] C.-H. Lambert, S. Mangin, B. S. D. C. S. Varaprasad, Y. K. Takahashi, M. Hehn, M. Cinchetti, G. Malinowski, K. Hono, Y. Fainman, M. Aeschlimann *et al.*, Science **345**, 1337 (2014).

[36] Y. Tokura and N. Kida, Phil. Trans. R. Soc. A **369**, 3679 (2011).

[37] A. Pimenov, A. A. Mukhin, V. Y. Ivanov, V. D. Travkin, A. M. Balbashov, and A. Loidl, Nat. Phys. **2**, 97 (2006).

[38] A. B. Sushkov, R. V. Aguilar, S. Park, S.-W. Cheong, and H. D. Drew, Phys. Rev. Lett. **98**, 027202 (2007).

[39] N. Kida, Y. Takahashi, J. S. Lee, R. Shimano, Y. Yamasaki, Y. Kaneko, S. Miyahara, N. Furukawa, T. Arima, and Y. Tokura, J. Opt. Soc. Am. B **26**, A35 (2009).

[40] P. Rovillain, R. de Sousa, Y. Gallais, A. Sacuto, M. A. Measson, D. Colson, A. Forget, M. Bibes, A. Barthelemy, and M. Cazayous, Nat. Mater. **9**, 975 (2010).

[41] A. Shuvaev, V. Dziom, A. Pimenov, M. Schiebl, A. A. Mukhin, A. C. Komarek, T. Finger, M. Braden, and A. Pimenov, Phys. Rev. Lett. **111**, 227201 (2013).

[42] S. Shastry, G. Srinivasan, M. I. Bichurin, V. M. Petrov, and A. S. Tatarenko, Phys. Rev. B **70**, 064416 (2004).

[43] J. Das, Y.-Y. Song, N. Mo, P. Krivosik, and C. E. Patton, Adv. Mater. **21**, 2045 (2009).

[44] J. Zhu, J. A. Katine, G. E. Rowlands, Y.-J. Chen, Z. Duan, J. G. Alzate, P. Upadhyaya, J. Langer, P. K. Amiri, K. L. Wang *et al.*, Phys. Rev. Lett. **108**, 197203 (2012).

[45] T. Nozaki, Y. Shiota, S. Miwa, S. Murakami, F. Bonell, S. Ishibashi, H. Kubota, K. Yakushiji, T. Saruya, A. Fukushima *et al.*, Nat. Phys. **8**, 491 (2012).

[46] A. N. Vasiliev and E. A. Popova, J. Low Temp. Phys. **32**, 735 (2006).

[47] A. M. Kadomtseva, Y. F. Popov, G. P. Vorob'ev, A. P. Pyatakov, S. S. Krotov, K. I. Kamilov, V. Y. Ivanov, A. A. Mukhin, A. K. Zvezdin, A. M. Kuz'menko *et al.*, J. Low Temp. Phys. **36**, 511 (2010).

[48] A. M. Kadomtseva, G. P. Vorob'ev, Y. F. Popov, A. P. Pyatakov, A. A. Mukhin, V. Y. Ivanov, A. K. Zvezdin, I. A. Gudim, V. L. Temerov, and L. N. Bezmaternykh, J. Exp. Theor. Phys. **114**, 810 (2012).

[49] J. A. Campá, C. Cascales, E. Gutirrez-Puebla, M. A. Monge, I. Rasines, and C. Ruz-Valero, Chem. Mater. **9**, 237 (1997).

[50] Y. Hinatsu, Y. Doi, K. Ito, M. Wakeshima, and A. Alemi, J. Solid State Chem. **172**, 438 (2003).

[51] D. Fausti, A. A. Nugroho, P. H. M. van Loosdrecht, S. A. Klimin, M. N. Popova, and L. N. Bezmaternykh, Phys. Rev. B **74**, 024403 (2006).

[52] M. N. Popova, Journal of rare earths / Chinese Society of Rare Earths **27**, 607 (2009).

[53] See Supplemental Material at http://link.aps.org/supplemental/10.1103/PhysRevLett.120.027203 for more details of experimental technique, properties of borates, and theoretical consideration.

[54] A. K. Zvezdin, G. P. Vorob'ev, A. M. Kadomtseva, Y. F. Popov, A. P. Pyatakov, L. N. Bezmaternykh, A. V. Kuvardin, and E. A. Popova, JETP Lett. **83**, 509 (2006).

[55] Y. F. Popov, A. P. Pyatakov, A. M. Kadomtseva, G. P. Vorob'ev, A. K. Zvezdin, A. A. Mukhin, V. Y. Ivanov, and I. A. Gudim, J. Exp. Theor. Phys. **111**, 199 (2010).

[56] A. A. Mukhin, G. P. Vorob'ev, V. Y. Ivanov, A. M. Kadomtseva, A. S. Narizhnaya, A. M. Kuz'menko, Y. F. Popov, L. N. Bezmaternykh, and I. A. Gudim, JETP Lett. **93**, 275 (2011).

[57] C. Ritter, A. Pankrats, I. Gudim, and A. Vorotynov, J. Phys. Condens. Matter **24**, 386002 (2012).

[58] A. I. Popov, D. I. Plokhov, and A. K. Zvezdin, Phys. Rev. B **87**, 024413 (2013).

[59] T. H. O'Dell, *The Electrodynamics of Magneto-electric Media* (North-Holland Publishing, Amsterdam, 1970).

[60] A. L. Freidman, A. D. Balaev, A. A. Dubrovskii, E. V. Eremin, K. A. Shaikhutdinov, V. L. Temerov, and I. A. Gudim, Phys. Solid State **57**, 1357 (2015).

[61] S. Partzsch, J.-E. Hamann-Borrero, C. Mazzoli, J. Herrero-Martin, S. Valencia, R. Feyerherm, E. Dudzik, A. Vasiliev, L. Bezmaternykh, B. Büchner *et al.*, Phys. Rev. B **94**, 054421 (2016).

[62] A. M. Kuz'menko, A. A. Mukhin, V. Y. Ivanov, A. M. Kadomtseva, and L. N. Bezmaternykh, JETP Lett. **94**, 294 (2011).

[63] A. M. Kuz'menko, A. A. Mukhin, V. Y. Ivanov, A. M. Kadomtseva, S. P. Lebedev, and L. N. Bezmaternykh, J. Exp. Theor. Phys. **113**, 113 (2011).

[64] A. M. Kuzmenko, A. Shuvaev, V. Dziom, A. Pimenov, M. Schiebl, A. A. Mukhin, V. Y. Ivanov, L. N. Bezmaternykh, and A. Pimenov, Phys. Rev. B **89**, 174407 (2014).

[65] A. M. Kuzmenko, V. Dziom, A. Shuvaev, A. Pimenov, M. Schiebl, A. A. Mukhin, V. Y. Ivanov, I. A. Gudim, L. N. Bezmaternykh, and A. Pimenov, Phys. Rev. B **92**, 184409 (2015).

[66] M. N. Popova, E. P. Chukalina, T. N. Stanislavchuk, B. Z. Malkin, A. R. Zakirov, E. Antic-Fidancev, E. A. Popova, L. N. Bezmaternykh, and V. L. Temerov, Phys. Rev. B **75**, 224435 (2007).

[67] E. P. Chukalina, M. N. Popova, L. N. Bezmaternykh, and I. A. Gudim, Phys. Lett. A **374**, 1790 (2010).

[68] A. A. Volkov, Y. G. Goncharov, G. V. Kozlov, S. P. Lebedev, and A. M. Prokhorov, Infrared Phys. **25**, 369 (1985).

[69] A. M. Kuzmenko, A. A. Mukhin, V. Y. Ivanov, G. A. Komandin, A. Shuvaev, A. Pimenov, V. Dziom, L. N. Bezmaternykh, and I. A. Gudim, Phys. Rev. B **94**, 174419 (2016).

[70] I. A. Gudim, A. I. Pankrats, E. I. Durnaĭkin, G. A. Petrakovskiı, L. N. Bezmaternykh, R. Szymczak, and M. Baran, Crystallogr. Rep. (Transl. Kristallografiya) **53**, 1140 (2008).

[71] A. A. Demidov, D. V. Volkov, I. A. Gudim, E. V. Eremein, and V. L. Temerov, J. Exp. Theor. Phys. **116**, 800 (2013).

[72] A. M. Kadomtseva, S. S. Krotov, Y. F. Popov, and G. P. Vorob'ev, J. Low Temp. Phys. **32**, 709 (2006).